Hindawi
Journal of Nanomaterials
Volume 2020, Article ID 1320274, 11 pages
https://doi.org/10.1155/2020/1320274

Research Article

Exploration of the Antimicrobial and Catalytic Properties of Gold Nanoparticles Greenly Synthesized by *Cryptolepis buchanani* Roem. and Schult Extract

Kamonpan Wongyai[1], **Phitchayapak Wintachai**[2], **Rasimate Maungchang**[3] and **Parawee Rattanakit**[1]

[1]*Department of Chemistry, School of Science, Walailak University, Nakhon Si Thammarat 80160, Thailand*
[2]*Department of Biology, School of Science, Walailak University, Nakhon Si Thammarat 80160, Thailand*
[3]*Department of Mathematics, School of Science, Walailak University, Nakhon Si Thammarat 80160, Thailand*

Correspondence should be addressed to Parawee Rattanakit; p_rattanakit@yahoo.com

Received 23 April 2020; Accepted 19 June 2020; Published 20 July 2020

Academic Editor: Takuya Tsuzuki

A green, simple, and rapid synthesis of gold nanoparticles using plant extract, *Cryptolepis buchanani* Roem. and Schult, and their applications are first described in this paper. The formation of gold nanoparticles was visually observed by the appearance of a ruby red color, which was further indicated by an absorption peak at 530 nm in UV-Vis spectroscopy. Optimization of reaction parameters for the gold nanoparticles was also investigated. Various analytical techniques were employed as part of the process of characterizing the resulting gold nanoparticles. Fourier transform infrared (FTIR) analysis revealed that the phenol compounds present in the extract were responsible for gold(III) reduction and stabilization of gold nanoparticles. Transmission electron microscopy (TEM) analysis showed that the gold nanoparticles were spherical in shape with an average diameter of 11 nm. Powder X-ray diffraction (XRD) pattern indicated that the green synthesis approach produced highly crystalline, face-centered cubic gold nanoparticles. Energy-dispersive X-ray spectroscopy (EDS) measurements confirmed the presence of elemental gold in the prepared nanoparticles. The negative zeta potential value of gold nanoparticles was found to be -30.28 mV. The green synthesized gold nanoparticles expressed effective antibacterial activity against *Staphylococcus aureus*, methicillin-resistant *Staphylococcus aureus*, and *Acinetobacter baumannii* and exhibited an excellent catalytic property in terms of its reduction ability of methylene blue.

1. Introduction

There has been a gradual emergence of investigation into the potential of metal nanoparticles in a variety of areas; this is due to their unique optical, electromagnetic, and area/volume properties [1, 2]. One of the most applicable metal nanoparticles is gold nanoparticles (AuNPs). Several synthetic pathways have been developed in order to produce metal nanoparticles [3–8]. Of these, conventional physical and chemical methods are commonly used as they provide uniform, stable, and size-controllable metal nanoparticles [9]. Nevertheless, the physical process has a high production cost since it requires high pressure and high energy during the synthesis procedure [10]. Also, toxic and hazardous chemicals are involved in the chemical process, affecting human health and the environment [11]. Therefore, finding an alternative biological synthesis approach is in demand, especially one that is simple, less expensive, and more environmentally friendly [5, 9, 12].

Extracts from plants are candidates for preparation of metal nanoparticles as part of the biological method due to their general availability, cost effectiveness, safety, shorter time of synthesis, and the ability to increase production volumes [13, 14]. Moreover, the use of natural resources often provides mild reaction conditions and *in situ* capping abilities. Active biocompounds found in plant extracts can act

as both reducing and stabilizing agents in the preparation of metal nanoparticles. Many research papers have reported on plant-mediated biosynthesis of metal nanoparticles. For AuNP synthesis, various plant extracts such as *Olea europaea* [15], *Ipomoea carnea* [16], *Salix alba* [17], *Genipa americana* [18], *Dalbergia coromandeliana* [19], *Piper longum* [20], *Eucommia ulmoides* bark [21], *Butea monosperma* [22], *Momordica charatia* [23], and *Lagerstroemia speciosa* [24] have been proposed. Polyphenolic, terpenoids, alkaloids, and sugars have been reported as being very well-known functional groups responsible for metal reducibility and nanoparticle stability [25]. Hence, plants that contain these groups may be utilized as biobased resources.

Cryptolepis buchanani Roem. and Schutt; *C. buchanani* (known as Thao-En-On in Thailand) is an indigenous plant which belongs to the Asclepiadaceae family [26]. It is widely used in folk medicine in Southeast Asia for treating muscle tension and arthritis [27]. The pharmacological properties of *C. buchanani* include antibacterial, anti-inflammatory, analgesic, chondroprotective, and hepatoprotective effects [28]. Bioactive phenolic compounds like flavonoids, alkaloids, saponins, and tannins are major phytochemicals found in the *C. buchanani* extract [28–30]. These phenolic groups participate in redox reactions by forming quinones, subsequently releasing electrons which reduce the number of gold ions (Au^{3+} to Au^{0}) and stabilize AuNPs [22, 31].

The aims of this study are to prepare the AuNPs with aqueous extract of *C. buchanani* and to assess their performance on the catalytic activity of methylene blue dye and antibacterial activities. To our best knowledge, using *C. buchanani* extract as a both reducing and stabilizing agents for the AuNP synthesis has not been previously detailed. Thus, this study is the first attempt to investigate the antimicrobial and catalytic properties of gold nanoparticles greenly synthesized by the *C. buchanani* extract.

2. Materials and Methods

2.1. Materials. All chemicals used in this study were of analytical reagent grade and deionized water was used throughout the reactions. All glasswares were washed with dilute nitric acid (HNO_3) and distilled water, then dried in an oven. A gold standard solution ($HAuCl_4$) of 1000 mg L^{-1} in 2 mol L^{-1} hydrochloric acid (HCl) was purchased from BDH (England). Sodium hydroxide (NaOH) was obtained from Loba Chemie Pvt. Ltd. (India). Methylene blue and sodium borohydride ($NaBH_4$) were purchased from Ajax Finechem (Australia).

2.2. Green Synthesis of AuNPs

2.2.1. Preparation of C. buchanani Aqueous Extract. Commercial *C. buchanani* tea powder was acquired from a local supermarket in Nakhon Si Thammarat Province, Thailand in 2019. Following a typical procedure, about 1 g of the *C. buchanani* powder was heated in 50 mL deionized water at 60°C for 15 min. After the solution was cooled, it was filtered through Whatman No.1 filter paper. The bright yellow filtrate was then kept in a refrigerator at 4°C. The extract was diluted to a final concentration of 60% (*v*/*v*) before usage.

2.2.2. Synthesis of AuNPs. The synthesis of AuNPs was performed using an aqueous solution of $HAuCl_4$ (1 mM) and *C. buchanani* extract in a 2 : 5 *v*/*v* ratio. After the gold solution was slowly added to the extract solution, the pH was adjusted to 7 using 0.1 M NaOH. It was then heated at 80°C for 30 min with continuous stirring. During this step, the emergence of a ruby red color indicated the formation of AuNPs.

2.3. Optimization of Reaction Parameters for the Green Synthesis of AuNPs. Experimental conditions used for the synthesis are essential since they affect the size, shape, yield, and agglomeration state of the nanoparticles [32]. Herein, different reaction parameters, including pH, reaction time, reaction temperature, and the concentration of $HAuCl_4$ and the extract were optimized using the univariate method.

The pH was studied over the range of 2-14 in order to investigate its effect on the AuNP synthesis. In order to evaluate the effect of temperature on the AuNP formation, the mixture temperature was controlled in a water bath at 40°C, 50°C, 60°C, 70°C, 80°C, 90°C, and 100°C for 30 min. The influence of reaction time was studied by monitoring the absorption spectra of the solution as a function of reaction time from 0 min to 80 min. The effect of $HAuCl_4$ concentration was optimized in the range of 1.25×10^{-4} to 7.5×10^{-4} M for biosynthesis reaction. The influence of various *C. buchanani* aqueous extract concentrations on the production of AuNPs was studied by increasing the concentration from 20 to 100 (% (*v*/*v*)). Absorption spectra of the AuNP formation were recorded in the range 450-750 nm with a UV-Vis spectrophotometer.

2.4. Characterizations of AuNPs. For UV-Vis spectroscopy, the reaction was monitored by recording the UV-Vis spectrum in wavelengths ranging from 450 to 750 nm by using a Jasco, V-630 spectrophotometer. Measurements of Fourier transform infrared spectroscopy (FTIR) were carried out with KBr disk using a Tensor 27, Bruker spectrometer in the range of 4,000-500 cm^{-1}. The elemental compositions of the synthesized AuNPs were investigated using an EDS (Zeiss Merlin Compact instrument) at an acceleration voltage of 10 kV. Transmission electron microscopy (TEM) images were collected on a JEOL TEM-2010 to analyse the size and morphology of the prepared AuNPs. The surface charge and stability of the AuNPs were measured by a Brookhaven ZetaPlus Zeta potential analyser. Crystalline metallic AuNPs were examined by an X-ray diffractometer (Rigaku, XtaLAB Supernova) operated at a voltage of 40 kV and a current of 30 mA using CuKα radiation. For the preparation of the solid samples, the colloidal AuNPs were centrifuged at 15,000 rpm for 30 min, washed twice with DI water, and dried at 60°C for 4 h in a vacuum oven before they were analysed.

2.5. Applications

2.5.1. Catalytic Degradation of Methylene Blue Dye. The catalytic activity of green synthesized AuNPs was demonstrated by degrading methylene blue (MB). Stock solutions of $NaBH_4$ and MB were freshly prepared before usage. MB

(1 mM, 200 μL) and $NaBH_4$ (0.1 M, 400 μL) were mixed in a quartz cuvette. Then, 50 μL of AuNPs was added, and the final volume was adjusted to 4 mL with the addition of deionized water. The reaction progress was monitored by UV-visible spectrophotometry in a range of 450 to 750 nm at room temperature. A control set was maintained without adding the AuNPs. The MB degradation percentage was calculated according to equation (1) below, where A_0 is the absorbance at $t = 0$ and A_t is the absorbance at time t.

$$\%D = \left(\frac{A_0 - A_t}{A_0}\right) \times 100. \quad (1)$$

2.5.2. MIC and MBC Determination. The antibacterial activity of the AuNPs towards three common bacterial pathogens, namely, *Staphylococcus aureus*, *methicillin-resistant Staphylococcus aureus*, and *Acinetobacter baumannii* was studied. Minimal inhibitory concentration (MIC) and minimal bactericidal concentration (MBC) were determined using a modified broth microdilution method which was adopted from [33]. Briefly, five colonies were diluted in the Mueller Hinton Broth (MBH) and cultured at 37°C for 7 h. Then, the bacterial suspension was adjusted to a final concentration of around 1×10^8 CFU/mL. One hundred microliters of bacterial suspension was added to the plate which contained 100 μL of serial twofold dilutions in MHB of AuNPs. The plates were incubated at 37°C for 16 h. Turbidity can be used to observe the growth of bacteria, and the MIC value was set at the lowest concentration that would prevent visible growth. To determine the MBC, 10 μL of the broth with the concentration of test material of MIC was dropped onto the Mueller Hinton Agar (MHA) plates before being incubated at 37°C for 16 h. The concentration that showed no bacteria growth was subsequently used as the MBC value. This experiment was undertaken independently in triplicate.

3. Results and Discussion

3.1. Optimizing Synthesis Parameters of AuNPs Formation. The effect of pH, temperature, *C. buchanani*, and precursor gold ion concentrations and reaction time were studied to find the optimum experimental conditions for the synthesis of AuNPs using the *C. buchanani* aqueous extract as reducing and stabilizing agents. In the present study, the optimum conditions were considered with regard to position, symmetry, and the narrowness or broadness of the surface plasmon resonance (SPR) band. The characteristics of the SPR band can indicate the qualities as well as quantities of the nanoparticles, i.e., morphology, size, and agglomeration [34]. Typically, a symmetrical and narrow SPR band indicates the presence of nanoparticles with a narrow range of size and that are uniform in shape. Other dominant factors are shifting or shape changes to the SPR band, increasing or decreasing of absorbance ability and changes to the maximum absorbance wavelength values [35].

3.1.1. Effect of pH. The pH value of the reaction solution has a critical impact on the morphology and size of the synthesized AuNPs. The synthesis of AuNPs in acidic, neutral, and alkaline conditions was carried out. As can be seen in Figure 1, the absorbance increases significantly as pH increases from 2 to 7, followed by a dramatic decrease in the pH from 8 to 14. In the acidic to neutral range, λ_{max} was observed at around 530 nm and the highest intensity was obtained at pH 7. In contrast to the alkaline condition, λ_{max} was shifted from 530 to 600 nm. It was observed that the nanoparticles aggregated to larger particles, resulting in a large shift in the SPR band [36]. Moreover, lower intensity and broadening SPR bands occurred when compared to acidic and neutral pH, indicating that the AuNPs formed inefficiently. A colorimetric visualization of the formed AuNPs at different pH levels is presented in Figure 1 (inset). It should be pointed out that different pH levels caused differently colored solutions. The light yellow of the *C. buchanani* extract solution turned into violet (pH 2 and 4), ruby red (pH 6-8), and black (pH 10-14) after mixing with the $HAuCl_4$. Unfortunately, the AuNPs were precipitated at pH 14. In general, the electric charges of biomolecules present in *C. buchanani* extract can be changed by altering the pH of the solution. This may affect both the capping and stabilizing ability, and subsequently, the growth of the nanoparticles [37, 38]. This study has revealed that a neutral pH is favorable for the content of the biomolecules in the extract to efficiently reduce and stabilize the AuNPs. Therefore, pH 7 was selected as the optimum pH for AuNP synthesis.

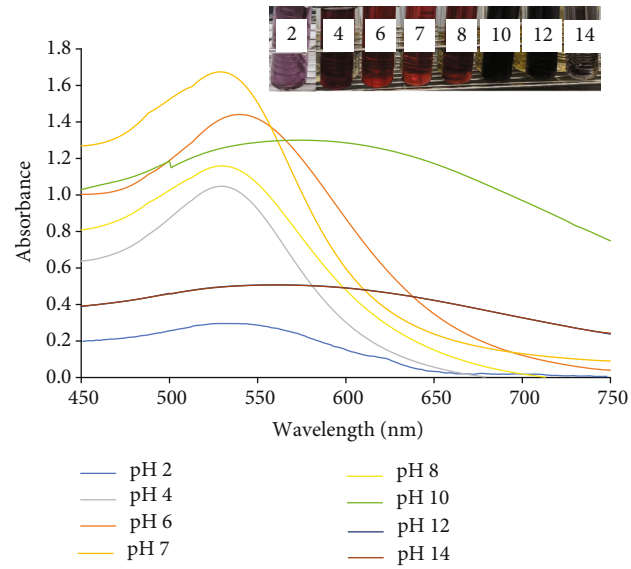

Figure 1: UV-Vis spectra of AuNPs at different pH values. The inset shows the photographic image of the colors of the AuNP solutions.

It should be noted that some previous studies have reported that a basic pH was favorable for AuNP production using various plant extracts such as olive leaf extract [39], Capsicum annuum var. grossum pulp extract [40], Momordica charantia fruit extract [23], and Lotus Leguminosae [41]. However, in this study, a neutral pH was found to be more favorable for the synthesis of AuNPs. The result is in a good agreement with [36] where AuNPs were synthesized using Dracocephalum kotschyi leaf extract.

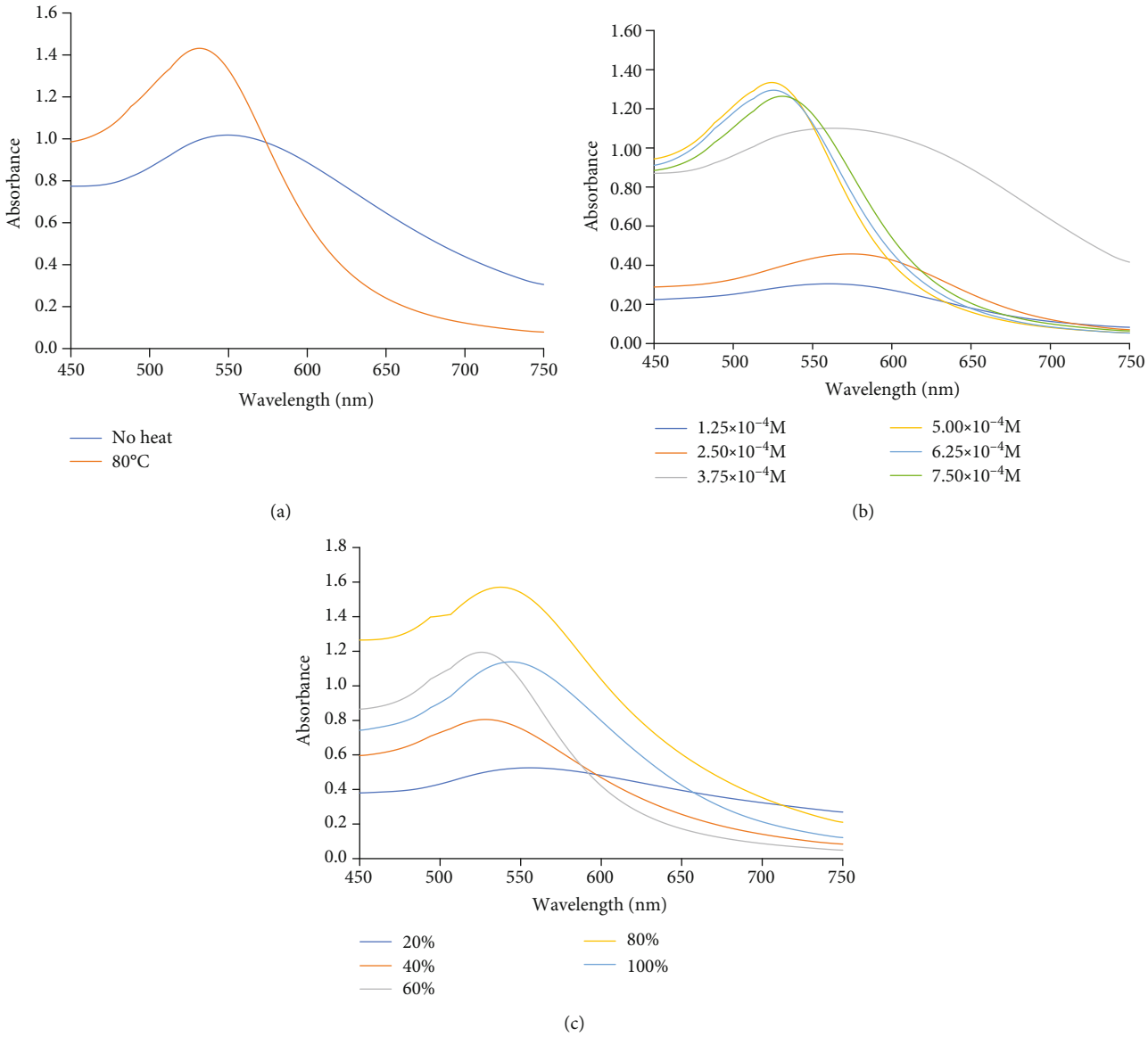

Figure 2: UV-Vis spectrum of green synthesized AuNPs prepared from *C. buchanani* aqueous extract (a) with and without heat treatment, (b) $HAuCl_4$ concentration, and (c) *C. buchanani* concentration.

3.1.2. Effect of Reaction Temperature and Time. In order to explore the impact of temperature on the AuNP formation, seven different temperatures were used in our experiment. As might be expected, the absorption intensity of AuNPs increased as temperature increased up to around about 80°C, above which it then started to slowly decrease. Thus, 80°C was applied as the optimal heating temperature for the preparation of AuNPs. The reaction times for the synthesis of the AuNPs (from 0 to 80 min) were also evaluated. The maximum absorbance value was saturated at 20 min, indicating the completion of the reduction process. However, the optimum reaction time selected for this study was 30 min. Figure 2(a) shows the UV-Vis absorption spectra which highlight the effect of heat treatment on the synthesis of AuNPs. The result demonstrated that the SPR peak of heated AuNPs increased significantly and became narrower; moreover, it appeared at a lower wavelength in comparison to the absorption peak of AuNPs prepared at room temperature. Increasing the reaction temperature from room temperature to 80°C decreased the formation time of the nanoparticles from 2 h to 20 min. Increasing the reaction temperature enhanced the formation rate of nanoparticles, resulting in the decrease of formation time [40] and formation of more small-sized nanoparticles [39].

3.1.3. Effect of $HAuCl_4$ Concentration. The formation of AuNPs was examined by adding different $HAuCl_4$ concentrations (1.25×10^{-4} to 7.5×10^{-4} M) to a constant concentration of the extract solution at 80°C for 30 min. The UV-Vis absorption spectra of the synthesized AuNPs at different

$HAuCl_4$ concentrations are presented in Figure 2(b). As the $HAuCl_4$ concentration increased, the shifts of the SPR band from 570 to 530 nm were observed. This indicates that the size of the nanoparticles decreased, resulting in them becoming more spherical in shape, as well as the distribution of the nanoparticles being more homogeneous [42, 43]. Additionally, the peaks at higher concentrations were seen to be more intense. Therefore, a concentration of 5.0 $\times 10^{-4}$ M $HAuCl_4$ was chosen as the optimum concentration for AuNP formation since it gave the highest absorption intensity.

3.1.4. Effect of Plant Extract Concentration. The effect of *C. buchanani* concentration on the synthesis of AuNPs was studied using different extract quantities (varying between 1 and 5 mL). The concentrations of the extract were 20-100% (*v*/*v*). Figure 2(c) shows the UV-Vis absorption spectra of greenly synthesized AuNPs using different concentrations of the extract. The absorption intensity gradually increased when the extract concentration increased from 20 to 60% (*v*/*v*). Besides, the absorption peak becomes sharper, and a blue shift was observed from 560 nm to 530 nm, suggesting a reduction in the mean diameter of the nanoparticles. However, when the concentration of the extract exceeded 60% (*v*/*v*), the absorption band became broader and shifted considerably back towards the red region, appearing at 540 and 550 nm for 80 and 100% (*v*/*v*), respectively. This is probably due to the rapid reduction of gold ions by large quantities of biomolecules or reducing agents [44]. Thus, the extract concentration at 60% (*v*/*v*) was chosen.

3.2. Characterization of Green Synthesized AuNPs. In this study, an aqueous extract of *C. buchanani* was utilized as a green reducing agent and stabilizer to synthesize AuNPs. The obtained AuNPs were characterized by employing UV-Vis spectroscopy, TEM, EDS, XRD, FTIR, and zeta potential techniques. The optimum conditions used for preparing the AuNPs were pH 7, 30 min reaction time, 80°C synthesis temperature, 60% (*v*/*v*) extract concentration, and 5×10^{-4} M $HAuCl_4$.

3.2.1. Visualizing the Formation of AuNPs and UV-Vis Spectrum Analysis. The ability of the aqueous *C. buchanani* extracts to produce AuNPs was firstly monitored by the naked eye and UV-Vis absorption spectroscopy. After adding a gold solution to the *C. buchanani* extract, the color of the solution changed from light yellow to ruby red while no change in color was observed in the absence of $HAuCl_4$ (Figure 3, inset). The appearance of the characteristic ruby red color indicates the reduction of Au^{3+} ions to gold nanoparticles. This visual observation could be attributed to the excitation of surface plasmon vibrations. Hence, it was used as a spectroscopic signature to show the formation of AuNPs. In general, the characteristic surface plasmon band from 500 to 550 nm indicates the spherical shape of AuNPs [45].

To retrieve information on the optical properties of the green synthesized AuNPs, the SPR was monitored by UV-Vis spectroscopy. The UV-Vis spectra of green synthesized AuNPs in which the SPR band was located at 530 nm confirmed the formation of spherical AuNPs in solution, as shown in Figure 3. This clearly demonstrates that the *C. buchanani* extract can perform as an excellent reducing and stabilizing agent for AuNP synthesis. Phytochemicals present in the *C. buchanani* extract such as flavonoid, alkaloids, saponins, and tannins are believed to play a key role in redox reactions by forming quinones and subsequently releasing electrons which reduce the number of gold ions (Au^{3+} to Au^0) and stabilize the AuNPs [46].

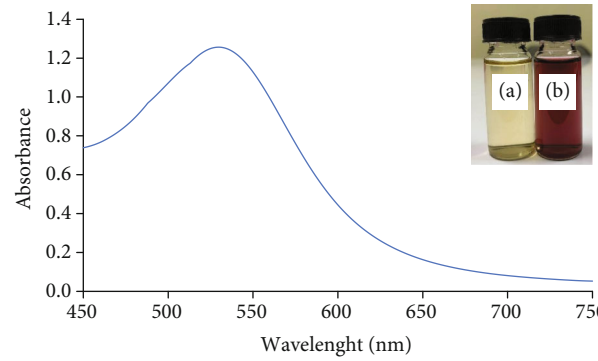

Figure 3: UV-Vis spectra of the green synthesized AuNPs using the *C. buchanani* extract. Inset: a digital image of the (a) *C. buchanani* extract solution and (b) AuNPs.

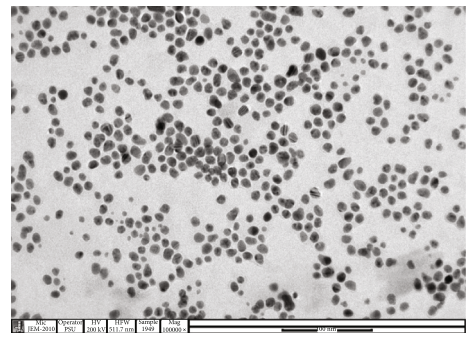

Figure 4: TEM image of the green synthesized AuNPs.

3.2.2. TEM Analysis and Zeta Potential. The morphology of the greenly synthesized AuNPs using the *C. buchanani* extract was examined using a TEM. Figure 4 shows that the dispersed AuNPs were spherical in shape with an average diameter of around 11.1 ± 1.3 nm. The zeta potential of the AuNPs was found to be -30.28 mV, indicating high stability, good colloidal nature, and high dispersibility due to negative-negative repulsion [47].

3.2.3. XRD and EDS Analysis. The crystalline characteristic of the synthesized AuNPs was determined by XRD analysis. Figure 5(a) shows the XRD pattern of AuNPs at 2θ ranging between 10° and 80°. Four characteristic diffraction peaks can be seen at two theta values of 38.02°, 44.9°, 65.26°, and 78.3°, which correspond to the (111), (200), (220), and

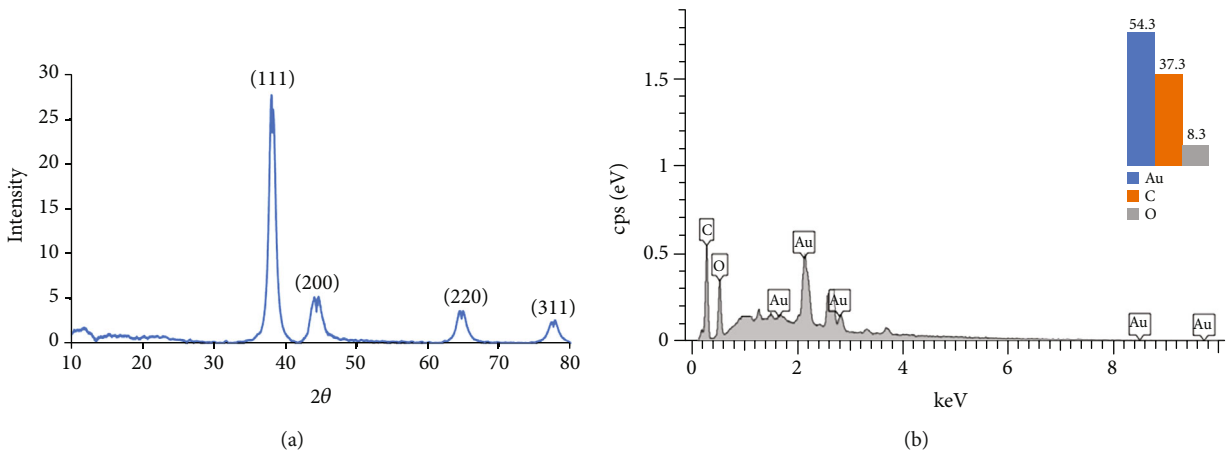

Figure 5: (a) XRD pattern and (b) EDS analysis of the synthesized AuNPs.

(311) planes of the face-centered cubic crystalline lattice of AuNPs, respectively. These peaks collaborated with the Joint Committee on Powder Diffraction Standard, JCPDS no. 04-0784 [48]. The peak corresponding to the (111) plane is more intense than the other planes, which indicates that (111) is the predominant orientation. The XRD spectrum strongly confirms the high crystalline nature of the prepared AuNPs. The elemental composition of the AuNPs was measured by EDS analysis. The presence of strong signals around 2 keV, as shown in Figure 5(b), confirmed the presence of metallic Au. The presence of C and O is due to the elemental composition of the *C. buchanani* extract [49].

3.2.4. FTIR Analysis. FTIR measurements were carried out to identify the potential functional groups of the biomolecules in the *C. buchanani* extract, which can be involved in the reduction of Au^{3+} and capping/stabilization of AuNPs. The major active components present in *C. buchanani* are known to be tannins, alkaloids, saponins, and flavonoids [28]. Figure 6 shows the FTIR spectra of the extract and the synthesized AuNPs. For the *C. buchanani* spectrum, the bands observed at 3419 and 2926 cm^{-1} are attributed to O-H and C-H stretching modes. The peak found at 1625 cm^{-1} is assigned to C=C and C=O stretching of the phytoconstituents. The strong absorption band at 1032 cm^{-1} corresponds to the vibration of the -C-O group of constituents. These observations indicate the presence of polyphenol in the extract. For FTIR spectra of the AuNPs, the characteristic absorption bands were found to be quite similar to those of the extract, but the vibration of the O-H group and the C=O group shifted from 3419 cm^{-1} to 3406 cm^{-1} and 1625 cm^{-1} to 1599 cm^{-1}, respectively. The small shifting and decreasing in intensities imply that the biomolecules in the extract, especially polyphenol, may be involved in facilitating the AuNPs, mainly through their oxygen functionalities. The results are in good agreement with those obtained by [50, 51]. All characterization results confirm that the aqueous extract of *C. buchanani* can be effectively used in the biosynthesis of the AuNPs.

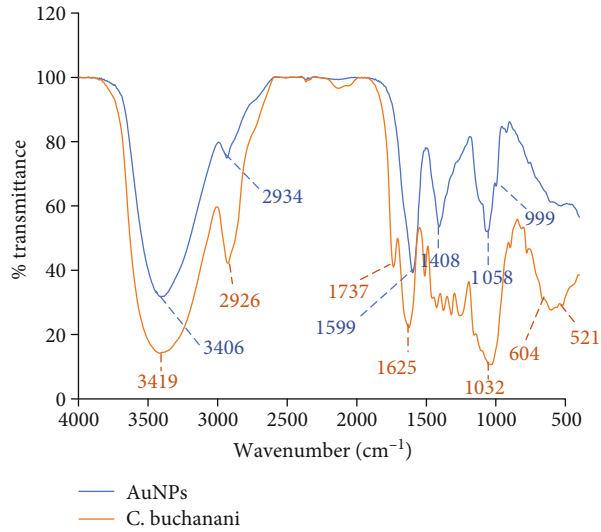

Figure 6: FTIR spectra of the synthesized AuNPs.

3.2.5. Comparison of the Properties of AuNPs Prepared with C. buchanani Extract with Select Previous Literature. The uses of various plant extracts for the green synthesis of AuNPs have been previously investigated in published studies, and the properties of the obtained AuNPs are listed in Table 1. As can be seen, different sizes and shapes of the prepared AuNPs are reported. The features of the produced AuNPs are dependent on the plant extracts and the reaction conditions. According to a careful examination of the synthesis conditions in this work, well-dispersed, small-sized AuNPs that had a uniform spherical shape were produced.

3.3. Applications

3.3.1. Catalytic Degradation of Methylene Blue. To evaluate the catalytic activity of the AuNPs synthesized by the *C. buchanani* extract, the reduction reaction of methylene blue (MB) dye by $NaBH_4$ was carried out as a model system. The experiment was conducted at room temperature, and the reactions were monitored by UV-visible spectroscopy.

Table 1: A partial list of the properties of AuNPs synthesized by plant extracts reported in the select literature.

Plant	Measurement technique	Size (nm)	Shape	ZP (mV)	Ref
Abutilon indicum	TEM	1-20	Sph	-25	[52]
Aegle marmelos		18			
Eugenia jambolana	TEM	28	Sph	—	[53]
Soursop		16			
Bacopa monnieri	TEM	3-45	Sph	—	[54]
Capsicum annuum var. *grossum*	TEM	6-37	Sph, Tri, Hex	—	[40]
Corchorus olitorius	TEM	27-35	Sph	—	[43]
Cornus mas	TEM	19	Sph	-33	[47]
Couroupita guianensis Aubl.	TEM	25 ± 6	Sph, Tri, Hex	—	[55]
C. buchanani	TEM	11	Sph	-30.3	This work
Croton caudatus geisel	TEM	20-50	Sph	—	[56]
Dalbergia coromandeliana	HRTEM	10.5	Sph	—	[19]
Dracocephalum kotschyi	TEM	8-23	Sph, Tri, Pen, Hex	-29.3	[36]
Elaeis guineensis	TEM	35-75	Sph, Tri, Pen	-17	[57]
Eucommia ulmoides	TEM	16.4	Sph	-21.3	[21]
Genipa americana	TEM	15-40	Sph	—	[18]
Hibiscus sabdariffa	TEM	10-60	Sph	—	[58]
Ipomoea carnea	TEM	3-100	Sph, Tri, Pen, Hex, R	—	[16]
Nepenthes khasiana	SEM	50-80	Tri, Sph	—	[59]
Nerium oleander	HRTEM	2-10	Sph	—	[60]
Olea europaea	TEM	50-100	Tri, hex, Sph	—	[39]
Justicia adhatoda	SEM	13-57	Sph	—	[61]
Sansevieria roxburghiana	TEM	5-31	Sph, Tri, Hex, Dec, R	—	[62]

Note: Dec: decahedral; Hex: hexagonal; Pen: pentagonal; R: rod; Sph: spherical; Tri: triangular; ZP: zeta potential.

Typically, an aqueous solution of MB imparting a blue color shows two characteristic absorption peaks at 664 nm with a shoulder at 612 nm [63]. The prominent band at 664 nm is assigned to the $n \rightarrow \pi^*$ transitions and a shoulder band at 612 nm is attributed to the dimer $(MB)^2$ due to its dimerization in aqueous medium [64]. When the prepared AuNPs were added to the reaction mixture containing MB dye and $NaBH_4$, the color of the dye gradually altered over time from deep blue to light blue before finally disappearing. The lack of color in the MB solution was due to the reduction of the MB to leucomethylene blue [65]. In the absence of catalyst AuNPs, no degradation of MB could be seen, although after 90 min of reaction between MB with a strong reducing agent, $NaBH_4$, it could be suggested that MB had not reduced effectively by $NaBH_4$ and reaction rate was very slow. When compared with the solution in the presence of the catalyst, the complete degradation (dye degradation at 95%) of MB was accomplished within 4 min (Figures 7(a) and 7(b)). The result proves that the *C. buchanani* extract-mediated AuNPs possess a significant catalytic activity.

A report on the catalytic mechanism of the degradation reaction of MB by AuNPs in the $NaBH_4$ system has been previously published [66]. Borohydride ions (BH_4^-) and the MB dye serve their roles as donors and an acceptor, respectively. The large redox potential difference between them kinetically hinders the reduction of dyes [67]. The AuNPs act as an electron relay and initiate shifting of the electrons from the BH_4^- ions (donor B_2H_4/BH_4^-) to the acceptor (acceptor LMB/MB), thus causing a reduction of the dye. BH_4^- ions are simultaneously adsorbed on the surface of the NPs; thus, electron transfer occurs from the BH_4^- ions to the dye through AuNPs [68].

According to the presence of excess reducing agent, the pseudofirst-order kinetic was applied herein. The slope of the linear regression plot of $\ln(A_0/A_t)$ versus reaction time, t, is the rate of degradation, which was found to be $0.3628\ min^{-1}$ (Figure 7(c)). The effect of the catalyst AuNP quantity on the degradation rate was also studied. The rate constant obtained from varying the volumes of the AuNPs is given in Table 2. The result shows that the rate constant increases with an increasing amount of AuNPs, suggesting that the reduction of MB occurs on the surface of the catalyst. A comparison of the catalytic activity of the AuNPs toward the degradation of MB is presented in Table 3. Additionally, the amounts of substrates (MB), reductants ($NaBH_4$), and catalysts (AuNPs) in each reduction of MB were carefully examined. The results obtained in our study are similar or superior to the reference presented in the last column of Table 3. The excellent catalytic efficiency of MB could be due to the small size of the synthesized AuNPs which plays an essential role in catalytic reduction of dye. Therefore, the greenly synthesized AuNPs using *C. buchanani* could act as

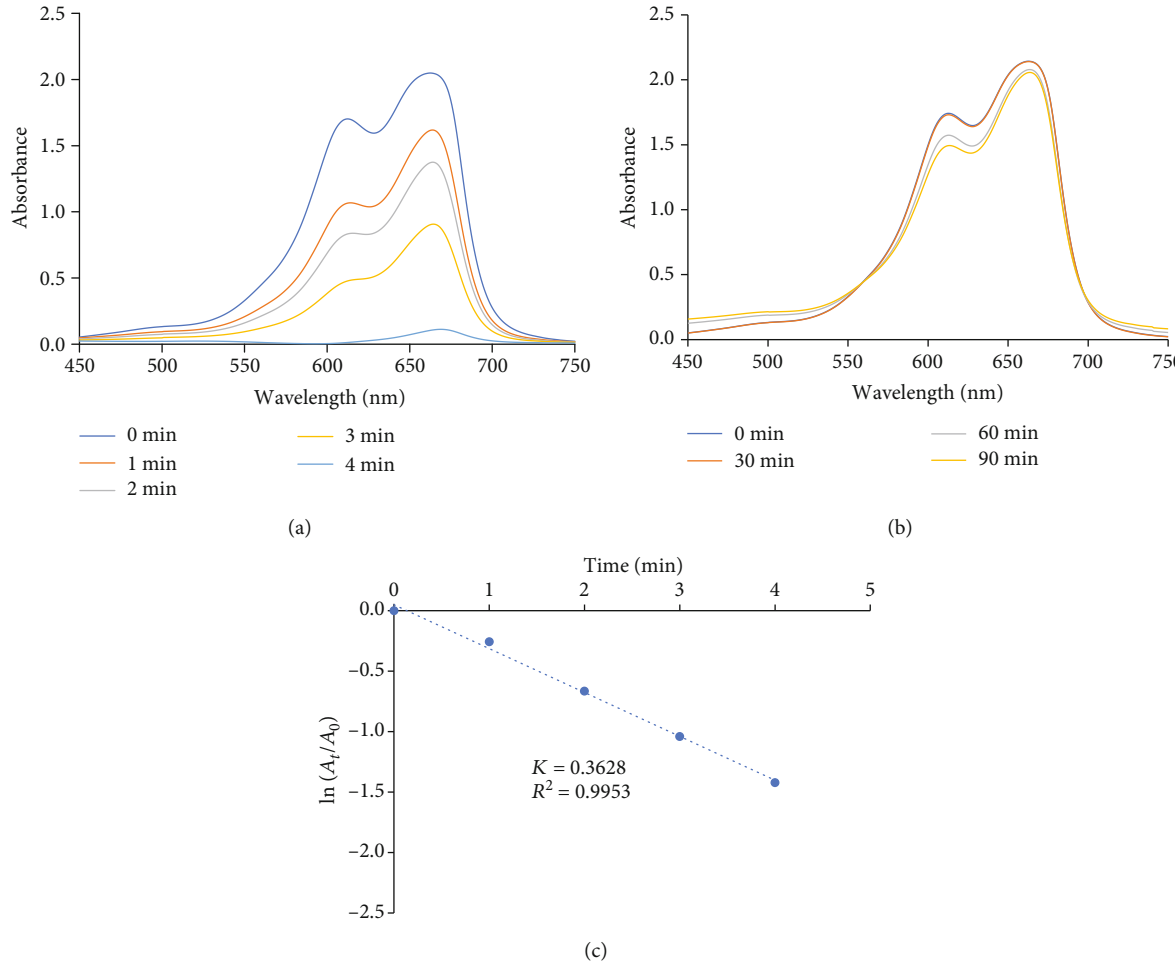

Figure 7: UV-visible spectra of reduction of MB by sodium borohydride in (a) the presence of AuNPs as the catalyst, (b) only $NaBH_4$, and (c) linear plot of MB over the time.

Table 2: The rate constant of different amount of AuNPs.

Volume of AuNP solution (μL)	Rate constant (min^{-1})
20	0.1634
30	0.2555
40	0.3398
50	0.3628

a promising material for the degradation of toxic MB dye and could be useful for developing organic dye-containing wastewater treatment.

3.3.2. Minimum Inhibitory Concentration (MIC) and Minimum Bactericidal Concentration (MBC). Generally, MIC and MBC values provide quantitative data on the antimicrobial efficacy of the AuNPs. The lowest AuNP concentration that inhibited visible growth of bacterial strains was defined as "MIC," whereas the lowest concentration of the AuNP that inhibited growth of ≥99.99% of bacterial strains was defined as "MBC.. The MIC and MBC values of *C. buchanani* extract mediating AuNPs were evaluated using a microbroth dilution method against *Staphylococcus aureus*, methicillin-resistant *Staphylococcus aureus*, and *Acinetobacter baumannii*. The results are shown in Table 4. The MIC values for all tested strains were equal to 0.209 μg/mL. The MBC values for *Staphylococcus aureus* and methicillin-resistant *Staphylococcus aureus* were both 0.418 μg/mL while a value greater than 0.835 μg/mL was observed for *Acinetobacter baumannii* (2-fold higher). According to the MBC values, Gram-positive bacteria exhibited higher sensitivity to that of Gram-negative bacteria. This might be due to the presence of capsules on the cell walls of bacteria, which prevent the attachment of the AuNPs [70]. Therefore, the biosynthesized AuNPs show significant potential in terms of their antimicrobial application.

4. Conclusions

Highly crystalline and monodispersed spherical AuNPs were successfully produced by using a rapid and straightforward green approach utilizing the *C. buchanani* aqueous extract. Using plant extract as reducing and stabilizing agents for synthesis offers advantages, such as the fact that plant extract

Table 3: Comparison of the catalytic activity of green synthesized AuNPs towards the degradation of MB.

($NaBH_4$) (M)	(MB) (mM)	AuNPs (μL)	AuNPs size (nm)	Degradation time (min)	Degradation (%)	Rate constant (min^{-1})	R^2	Ref.
0.15	1	100	17	60	49.62	0.0118	0.9852	[62]
0.03	1	1000	≤40	14	>90	0.1980	0.9600	[24]
0.05	0.1	100	11	8	95.62	0.0720	0.9786	[69]
0.1	1	50	11	4	94.81	0.3628	0.9953	This work

Table 4: MIC and MBC values of the AuNPs against the three pathogenic strains.

Test organisms	Gram class	MIC (μg/mL)	MBC (μg/mL)
Staphylococcus aureus	Gram positive	0.209	0.418
Methicillin-resistant *Staphylococcus aureus*	Gram positive	0.209	0.418
Acinetobacter baumannii	Gram negative	0.209	>0.835

is readily available, sustainable, ecofriendly, cost effective, and nonhazardous. The prepared AuNPs exhibited efficient antimicrobial activities against both Gram-positive and Gram-negative bacteria. Moreover, they were also proven as efficient catalysts with enhanced rates of reduction of MB dye. Therefore, the green synthesized AuNPs are potentially useful for environmental remediation applications.

Data Availability

All data supporting the findings of this study are available within the article. The data that support the findings of this study (TEM images, EDS analysis, and XRD patterns) are available from the corresponding author upon request.

Conflicts of Interest

The authors declare no conflict of interest.

Acknowledgments

This research was funded by the Walailak University, grant numbers WU_IRG61_20, Master Degree Excellent Scholarships 02/2561, and WU 19/2562.

References

[1] W. J. Keijok, R. H. A. Pereira, L. A. C. Alvarez et al., "Controlled biosynthesis of gold nanoparticles with *Coffea arabica* using factorial design," *Scientific Reports*, vol. 9, no. 1, p. 16019, 2019.

[2] A. Henglein, "Physicochemical properties of small metal particles in solution: "microelectrode" reactions, chemisorption, composite metal particles, and the atom-to-metal transition," *Journal of Physical Chemistry.*, vol. 97, no. 21, pp. 5457–5471, 1993.

[3] M. Shariq, B. Friedrich, B. Budic et al., "Successful synthesis of gold nanoparticles through ultrasonic spray pyrolysis from a gold(III) nitrate precursor and their interaction with a high electron beam," *ChemistryOpen*, vol. 7, no. 7, pp. 533–542, 2018.

[4] I. Ojea-Jimenez, F. M. Romero, N. G. Bastus, and V. Puntes, "Small gold nanoparticles synthesized with sodium citrate and heavy water: insights into the reaction mechanism," *Journal of Physical Chemistry C*, vol. 114, no. 4, pp. 1800–1804, 2010.

[5] V. V. Makarov, A. J. Love, O. V. Sinitsyna et al., ""Green" nanotechnologies: synthesis of metal nanoparticles using plants," *Acta Naturae*, vol. 6, no. 1, pp. 35–44, 2014.

[6] B. Sharma, D. D. Purkayastha, S. Hazra et al., "Biosynthesis of gold nanoparticles using a freshwater green alga, Prasiola crispa," *Materials Letters*, vol. 116, pp. 94–97, 2014.

[7] S. He, Z. Guo, Y. Zhang, S. Zhang, J. Wang, and N. Gu, "Biosynthesis of gold nanoparticles using the bacteria *Rhodopseudomonas capsulata*," *Materials Letters*, vol. 61, no. 18, pp. 3984–3987, 2007.

[8] I. Willner, R. Baron, and B. Willner, "Growing metal nanoparticles by enzymes," *Advanced Materials*, vol. 18, no. 9, pp. 1109–1120, 2006.

[9] C. Dhand, N. Dwivedi, X. J. Loh et al., "Methods and strategies for the synthesis of diverse nanoparticles and their applications: a comprehensive overview," *RSC Advances*, vol. 5, no. 127, pp. 105003–105037, 2015.

[10] S. Taheriniya and Z. Behboodi, "Comparing green chemical methods and chemical methods for the synthesis of titanium dioxide nanoparticles," *International Journal of Pharmaceutical Sciences Research*, vol. 7, pp. 4927–4932, 2016.

[11] R. Herizchi, E. Abbasi, M. Milani, and A. Akbarzadeh, "Current methods for synthesis of gold nanoparticles," *Artificial Cells, Nanomedicine, and Biotechnology*, vol. 44, no. 2, pp. 596–602, 2014.

[12] Z. Zhang, J. Wang, X. Nie et al., "Near infrared laser-induced targeted cancer therapy using thermoresponsive polymer encapsulated gold nanorods," *Journal of the American Chemical Society*, vol. 136, no. 20, pp. 7317–7326, 2014.

[13] J. Singh, T. Dutta, K. H. Kim, M. Rawat, P. Samddar, and P. Kumar, "'Green' synthesis of metals and their oxide nanoparticles: applications for environmental remediation," *Journal of Nanobiotechnology*, vol. 16, no. 1, 2018.

[14] O. V. Kharissova, H. V. R. Dias, B. I. Kharisov, B. O. Pérez, and V. M. J. Pérez, "The greener synthesis of nanoparticles," *Trends in Biotechnology.*, vol. 31, no. 4, pp. 240–248, 2013.

[15] A. M. Awwad, N. M. Salem, and A. O. Abdeen, "Biosynthesis of silver nanoparticles using *Olea europaea* leaves extract and its antibacterial activity," *Nanoscience and Nanotechnology*, vol. 2, no. 6, pp. 164–170, 2012.

[16] T. Abbasi, J. Anuradha, S. U. Ganaie, and S. A. Abbasi, "Gainful utilization of the highly intransigent weed ipomoea in the synthesis of gold nanoparticles," *Journal of King Saud University - Science*, vol. 27, no. 1, pp. 15–22, 2015.

[17] N. U. Islam, K. Jalil, M. Shahid et al., "Green synthesis and biological activities of gold nanoparticles functionalized with *Salix alba*," *Arabian Journal of Chemistry.*, vol. 12, no. 8, pp. 2914–2925, 2019.

[18] B. Kumar, K. Smita, L. Cumbal et al., "One pot phytosynthesis of gold nanoparticles using *Genipa americana* fruit extract and its biological applications," *Materials Science and Engineering: C*, vol. 62, pp. 725–731, 2016.

[19] C. Umamaheswari, A. Lakshmanan, and N. S. Nagarajan, "Green synthesis, characterization and catalytic degradation studies of gold nanoparticles against Congo red and methyl orange," *Journal of Photochemistry and Photobiology B: Biology*, vol. 178, pp. 33–39, 2018.

[20] J. R. Nakkala, R. Mata, and S. R. Sadras, "The antioxidant and catalytic activities of green synthesized gold nanoparticles from *Piper longum* fruit extract," *Process Safety and Environmental Protection*, vol. 100, pp. 288–294, 2016.

[21] M. Guo, W. Li, F. Yang, and H. Liu, "Controllable biosynthesis of gold nanoparticles from a *Eucommia ulmoides* bark aqueous extract," *Spectrochimica Acta-Part A: Molecular and Biomolecular Spectroscopy*, vol. 142, pp. 73–79, 2015.

[22] S. Patra, S. Mukherjee, A. K. Barui, A. Ganguly, B. Sreedhar, and C. R. Patra, "Green synthesis, characterization of gold and silver nanoparticles and their potential application for cancer therapeutics," *Materials Science and Engineering: C*, vol. 53, pp. 298–309, 2015.

[23] K. Singh, D. Kukkar, R. Singh, P. Kukkar, and K. H. Kim, "Exceptionally stable green-synthesized gold nanoparticles for highly sensitive and selective colorimetric detection of trace metal ions and volatile aromatic compounds," *Journal of Industrial and Engineering Chemistry*, vol. 68, pp. 33–41, 2018.

[24] B. C. Choudhary, D. Paul, T. Gupta et al., "Photocatalytic reduction of organic pollutant under visible light by green route synthesized gold nanoparticles," *Journal of Environmental Sciences*, vol. 55, pp. 236–246, 2017.

[25] M. K. Choudhary, J. Kataria, and S. Sharma, "A biomimetic synthesis of stable gold nanoparticles derived from aqueous extract of *Foeniculum vulgare* seeds and evaluation of their catalytic activity," *Applied Nanoscience*, vol. 7, no. 7, pp. 439–447, 2017.

[26] P. Laupattarakasem, T. Wangsrimongkol, R. Surarit, and C. Hahnvajanawong, "*In vitro* and *in vivo* anti-inflammatory potential of *Cryptolepis buchanani*," *Journal of Ethnopharmacology*, vol. 108, no. 3, pp. 349–354, 2006.

[27] N. Hanprasertpong, S. Teekachunhatean, R. Chaiwongsa et al., "Analgesic, anti-inflammatory, and chondroprotective activities of *Cryptolepis buchanani* extract: *in vitro* and *in vivo* studies," *BioMed Research International*, vol. 2014, Article ID 978582, 8 pages, 2014.

[28] K. S. Vinayaka, K. T. R. Prashith, N. Mallikarjun, and V. N. Sateesh, "Anti-dermatophyte activity of *Cryptolepis buchanani* Roem. & Schult," *Pharmacognosy Journal*, vol. 2, no. 7, pp. 170–172, 2010.

[29] K. Sunil, D. Batuk, N. Sharma, and P. V. Sharria, "A new nicotinoyl glucoside from *Cryptolepis buchanani*," *Phytochemistry*, vol. 19, no. 6, p. 1278, 1980.

[30] S. K. Dutta, B. N. Sharma, and P. V. Shakma, "Buchananine, a novel pyridine alkaloid from _Cryptolepis buchanani_," *Phytochemistry*, vol. 17, no. 11, pp. 2047-2048, 1978.

[31] T. Ahmad, "Reviewing the tannic acid mediated synthesis of metal nanoparticles," *Journal of Nanotechnology*, vol. 2014, Article ID 954206, 11 pages, 2014.

[32] G. Arya, R. M. Kumari, N. Gupta, A. Kumar, R. Chandra, and S. Nimesh, "Green synthesis of silver nanoparticles usingProsopis juliflorabark extract: reaction optimization, antimicrobial and catalytic activities," *Artificial Cells, Nanomedicine, and Biotechnology*, vol. 46, no. 5, pp. 985–993, 2017.

[33] P. Wintachai, S. Paosen, C. T. Yupanqui, and S. P. Voravuthikunchai, "Silver nanoparticles synthesized with *Eucalyptus critriodora* ethanol leaf extract stimulate antibacterial activity against clinically multidrug-resistant *Acinetobacter baumannii* isolated from pneumonia patients," *Microbial Pathogenesis*, vol. 126, pp. 245–257, 2019.

[34] O. Velgosova, A. Mrazikova, and R. Marcincakova, "Influence of pH on green synthesis of Ag nanoparticles," *Materials Letters*, vol. 180, pp. 336–339, 2016.

[35] S. Sohrabnezhad, M. Rassa, and A. Seifi, "Green synthesis of Ag nanoparticles in montmorillonite," *Materials Letters*, vol. 168, pp. 28–30, 2016.

[36] N. Dorosti and F. Jamshidi, "Plant-mediated gold nanoparticles by *Dracocephalum kotschyi* as anticholinesterase agent: synthesis, characterization, and evaluation of anticancer and antibacterial activity," *Journal of Applied Biomedicine*, vol. 14, no. 3, pp. 235–245, 2016.

[37] M. M. H. Khalil, E. H. Ismail, K. Z. El-Baghdady, and D. Mohamed, "Green synthesis of silver nanoparticles using olive leaf extract and its antibacterial activity," *Arabian Journal of Chemistry*, vol. 7, no. 6, pp. 1131–1139, 2014.

[38] A. Verma and M. S. Mehata, "Controllable synthesis of silver nanoparticles using Neem leaves and their antimicrobial activity," *Journal of Radiation Research and Applied Sciences*, vol. 9, no. 1, pp. 109–115, 2019.

[39] M. M. H. Khalil, E. H. Ismail, and F. El-Magdoub, "Biosynthesis of Au nanoparticles using olive leaf extract," *Arabian Journal of Chemistry*, vol. 5, no. 4, pp. 431–437, 2012.

[40] C.-G. Yuan, C. Huo, S. Yu, and B. Gui, "Biosynthesis of gold nanoparticles using *Capsicum annuum* var. *grossum* pulp extract and its catalytic activity," *Physica E: Low-dimensional Systems and Nanostructures*, vol. 85, pp. 19–26, 2017.

[41] M. H. Oueslati, L. B. Tahar, and A. H. Harrath, "Catalytic, antioxidant and anticancer activities of gold nanoparticles synthesized by kaempferol glucoside from *Lotus leguminosae*," *Arabian Journal of Chemistry*, vol. 13, no. 1, pp. 3112–3122, 2020.

[42] K. A. Eid and H. M. Azzazy, "Sustained broad-spectrum antibacterial effects of nanoliposomes loaded with silver nanoparticles," *Nanomedicine*, vol. 9, no. 9, pp. 1301–1310, 2014.

[43] E. Ismail, A. Saqer, E. Assirey, A. Naqvi, and R. Okasha, "Successful green synthesis of gold nanoparticles using a *Corchorus olitorius* extract and their antiproliferative effect in cancer cells," *International Journal of Molecular Sciences*, vol. 19, no. 9, pp. 2612–2614, 2018.

[44] M. Shaik, M. Khan, M. Kuniyil et al., "Plant-extract-assisted green synthesis of silver nanoparticles using *Origanum vulgare*

L. extract and their microbicidal activities," *Sustainability*, vol. 10, no. 4, p. 913, 2018.

[45] M. A. Fuller and I. Koper, "Biomedical applications of polyelectrolyte coated spherical gold nanoparticles," *Nano Convergence*, vol. 6, no. 1, p. 11, 2019.

[46] R. Majumdar, B. G. Bag, and N. Maity, "*Acacia nilotica* (Babool) leaf extract mediated size-controlled rapid synthesis of gold nanoparticles and study of its catalytic activity," *International Nano Letters*, vol. 3, no. 1, pp. 1–6, 2013.

[47] G. A. Filip, B. Moldovan, I. Baldea et al., "UV-light mediated green synthesis of silver and gold nanoparticles using Cornelian cherry fruit extract and their comparative effects in experimental inflammation," *Journal of Photochemistry & Photobiology, B: Biology*, vol. 191, pp. 26–37, 2019.

[48] L. Cheng, X. Li, and J. Dong, "Size-controlled preparation of gold nanoparticles with novel pH responsive gemini amphiphiles," *Journal of Materials Chemistry C*, vol. 3, no. 24, pp. 6334–6340, 2015.

[49] J. Li, Q. Li, X. Ma et al., "Biosynthesis of gold nanoparticles by the extreme bacterium *Deinococcus radiodurans* and an evaluation of their antibacterial properties," *International Journal of Nanomedicine*, vol. Volume 11, pp. 5931–5944, 2016.

[50] T. N. J. I. Edison, Y. R. Lee, and M. G. Sethuraman, "Green synthesis of silver nanoparticles using _Terminalia cuneata_ and its catalytic action in reduction of direct yellow-12 dye," *Spectrochimica Acta Part A: Molecular and Biomolecular Spectroscopy*, vol. 161, pp. 122–129, 2016.

[51] N. A. Khan, A. Niaz, M. I. Zaman, F. A. Khan, M. Nisar-ul-haq, and M. Tariq, "Sensitive and selective colorimetric detection of Pb^{2+} by silver nanoparticles synthesized from _Aconitum violaceum_ plant leaf extract," *Materials Research Bulletin*, vol. 102, pp. 330–336, 2018.

[52] R. Mata, J. R. Nakkala, and S. R. Sadras, "Polyphenol stabilized colloidal gold nanoparticles from *Abutilon indicum* leaf extract induce apoptosis in HT-29 colon cancer cells," *Colloids and Surfaces B: Biointerfaces*, vol. 143, pp. 499–510, 2016.

[53] S. Vijayakumar, "Eco-friendly synthesis of gold nanoparticles using fruit extracts and *in vitro* anticancer studies," *Journal of Saudi Chemical Society*, vol. 23, no. 6, pp. 753–761, 2019.

[54] P. J. Babu, P. Sharma, S. Saranya, and U. Bora, "Synthesis of gold nanoparticles using ethonolic leaf extract of *Bacopa monnieri* and UV irradiation," *Materials Letters*, vol. 93, pp. 431–434, 2013.

[55] G. Sathishkumar, P. K. Jha, V. Vignesh et al., "Cannonball fruit (*Couroupita guianensis* , Aubl.) extract mediated synthesis of gold nanoparticles and evaluation of its antioxidant activity," *Journal of Molecular Liquids*, vol. 215, pp. 229–236, 2016.

[56] P. V. Kumar, S. M. J. Kala, and K. S. Prakash, "Green synthesis of gold nanoparticles using _Croton Caudatus Geisel_ leaf extract and their biological studies," *Materials Letters*, vol. 236, pp. 19–22, 2019.

[57] T. Ahmad, M. A. Bustam, M. Irfan, M. Moniruzzaman, H. M. A. Asghar, and S. Bhattacharjee, "Green synthesis of stabilized spherical shaped gold nanoparticles using novel aqueous *Elaeis* guineensis (oil palm) leaves extract," *Journal of Molecular Structure*, vol. 1159, pp. 167–173, 2018.

[58] P. Mishra, S. Ray, S. Sinha et al., "Facile bio-synthesis of gold nanoparticles by using extract of _Hibiscus sabdariffa_ and evaluation of its cytotoxicity against U87 glioblastoma cells under hyperglycemic condition," *Biochemical Engineering Journal*, vol. 105, pp. 264–272, 2016.

[59] B. S. Bhau, S. Ghosh, S. Puri, B. Borah, D. K. Sarmah, and R. Khan, "Green synthesis of gold nanoparticles from the leaf extract of *Nepenthes khasiana* and antimicrobial assay," *Advanced Materials Letters*, vol. 6, no. 1, pp. 55–58, 2015.

[60] K. Tahir, S. Nazir, B. Li et al., "*Nerium oleander* leaves extract mediated synthesis of gold nanoparticles and its antioxidant activity," *Materials Letters*, vol. 156, pp. 198–201, 2015.

[61] D. Latha, S. Sampurnam, C. Arulvasu, P. Prabu, K. Govindaraju, and V. Narayanan, "Biosynthesis and characterization of gold nanoparticle from *Justicia adhatoda* and its catalytic activity," *Materials Today: Proceedings*, vol. 5, no. 2, pp. 8968–8972, 2018.

[62] I. Kumar, M. Mondal, V. Meyappan, and N. Sakthivel, "Green one-pot synthesis of gold nanoparticles using _Sansevieria roxburghiana_ leaf extract for the catalytic degradation of toxic organic pollutants," *Materials Research Bulletin*, vol. 117, pp. 18–27, 2019.

[63] N. Y. Nadaf and S. S. Kanase, "Biosynthesis of gold nanoparticles by *Bacillus marisflavi* and its potential in catalytic dye degradation," *Arabian Journal of Chemistry*, vol. 12, no. 8, pp. 4806–4814, 2019.

[64] U. P. Azad, V. Ganesan, and M. Pal, "Catalytic reduction of organic dyes at gold nanoparticles impregnated silica materials: influence of functional groups and surfactants," *Journal of Nanoparticle Research*, vol. 13, no. 9, pp. 3951–3959, 2011.

[65] N. Cheval, N. Gindy, C. Flowkes, and A. Fahmi, "Polyamide 66 microspheres metallised with *in situ* synthesised gold nanoparticles for a catalytic application," *Nanoscale Research Letters*, vol. 7, no. 1, pp. 182–189, 2012.

[66] B. Paul, B. Bhuyan, D. D. Purkayastha, M. Dey, and S. S. Dhar, "Green synthesis of gold nanoparticles using *Pogestemon benghalensis (B) O. Ktz*. leaf extract and studies of their photocatalytic activity in degradation of methylene blue," *Materials Letters*, vol. 148, pp. 37–40, 2015.

[67] N. Sreeju, A. Rufus, and D. Philip, "Microwave-assisted rapid synthesis of copper nanoparticles with exceptional stability and their multifaceted applications," *Journal of Molecular Liquids*, vol. 221, pp. 1008–1021, 2016.

[68] M. M. Kumari, J. Jacob, and D. Philip, "Green synthesis and applications of Au-Ag bimetallic nanoparticles," *Spectrochimica Acta Part A: Molecular and Biomolecular Spectroscopy*, vol. 137, pp. 185–192, 2015.

[69] P. Narasaiah, B. K. Mandal, and S. N. Chakravarthula, "Synthesis of gold nanoparticles by cotton peels aqueous extract and their catalytic efficiency for the degradation of dyes and antioxidant activity," *IET Nanobiotechnology*, vol. 12, no. 2, pp. 156–165, 2018.

[70] M. P. Patil, R. D. Singh, P. B. Koli et al., "Antibacterial potential of silver nanoparticles synthesized using _Madhuca longifolia_ flower extract as a green resource," *Microbial Pathogenesis*, vol. 121, pp. 184–189, 2018.